NUMERICAL TECHNIQUES TO DETERMINE THE UTD BISTATIC CREEPING WAVE PATHS AND PARAMETERS FOR AN ELLIPSOID *

Jaehoon Choi
Arizona State University Telecommunications Research Center
Tempe, AZ 85287-7206

and

Ronald J. Marhefka
The Ohio State University ElectroScience Laboratory
Columbus, Ohio 43212-1191

Abstract

In applying the Uniform Geometrical Theory of Diffraction (UTD) to evaluate the scattering patterns of a doubly curved surface, the determination of correct ray paths is one of the most important and difficult tasks. In this paper, an efficient numerical technique to obtain the complete ray path of the creeping wave for the bistatic scattering of an ellipsoid is discussed. Also, the numerical method to evaluate the energy spreading factor of the creeping wave and the caustic distance at the diffraction (launching) point are described. An ellipsoid is chosen because of its modeling capability to represent the fuselage of an aircraft and similar objects. The same numerical techniques for an ellipsoid can be extended to a general doubly curved surface as well.

*This work was supported by Naval Weapons Center under contract No. N60530-85-C-0249

I. Introduction

When the receiver is in the shadow region of an incident ray, or in the lit region where the rays do not travel a long way around the surface, the surface creeping wave fields can provide a significant contribution to the total field. Since the creeping wave in the UTD [1] expression is related to the parameters of the scatterer's surface, it is necessary to have knowledge about the differential geometry [2] of a scatterer and to find the geodesic paths on the given surface. In general, it is a difficult time consuming task to find the creeping wave paths for a given source and receiver location.

Efficient numerical techniques to evaluate the complete ray path from the source to the surface geodesic then to the receiver location, the energy spreading factor for the creeping wave, and the caustic distance at the diffraction point are developed in this paper. Barger's algorithm [3] for the geodesic path on a general surface is adopted in this study to trace the ray path on the ellipsoid surface. The present results are compared with those of an alternative method [4].

In order to find the complete creeping wave ray path, both the attaching (grazing) point and the launching (diffraction) point pairs for a given source and receiver location need to be determined. To find the attaching points for a given scattering direction, one can use the tangential arc on an ellipsoid which is defined by a zero dot product of the surface normal vector and incident unit vector from the source to the ellipsoid's surface. Once the tangential arc on the ellipsoid is determined, a potential starting point on the tangential arc can be chosen with its initial condition of the tangential starting direction by which a unique geodesic path is defined. Having the starting point and tangential starting direction, the differential form of the geodesic equation can be solved in a numerical way. After making a small incremental step along the geodesic path, it is necessary to test whether the geodesic tangent vector will point directly at the receiver location or not. The same procedure is repeated for the subsequent attaching points along the tangential arc for the given source and receiver until all the possible attaching and launching point pairs are found. Usually there are four ray paths for the given source and receiver pairs. Once all the attaching and launching point pairs and the corresponding geodesic paths are found, the energy spreading factor for the creeping wave and the caustic distance at the launching point are determined numerically.

Once the attaching (grazing) and corresponding launching (diffraction) point pairs for the given receiver location are known, the receiver is assumed to move a small amount,

then the new attaching and launching point pairs for the new receiver location can be found by utilizing a bisectional search technique. If the receiver goes into (or comes out of) the shadow region, or goes through a caustic region, the start-up algorithm mentioned in the previous paragraph needs to be reinitiated.

In the following sections, a numerical method to determine the ray paths based on the differential form of the geodesic equation is described. Also, the numerical evaluation of the energy spreading factor and the caustic distance at the launching point are presented. Some numerical examples of the geodesic paths on an ellipsoid are given for bistatic scattering. The full analysis of the UTD approach for bistatic scattering of an ellipsoid are available in Reference [5,6], it is not repeated in this paper.

II. Geodesic Path on an Ellipsoid

The surface of an ellipsoid, illustrated in Figure 1, is given in vector parametric notation as

$$\bar{R} = a \sin u \cos v \hat{x} + b \sin u \sin v \hat{y} + c \cos u \hat{z} \tag{1}$$

where u and v are the two elliptic parameters defined as shown in Figure 1, and their definitions are similar to those of θ and ϕ of the spherical coordinate system. In general, the geodesic equation (Reference [2], pg. 234) must satisfy

$$\frac{d^2u}{ds^2} + \Gamma_{11}^1 (\frac{du}{ds})^2 + 2\Gamma_{12}^1 \frac{du}{ds}\frac{dv}{ds} + \Gamma_{22}^1 (\frac{dv}{ds})^2 = 0, \tag{2}$$

and

$$\frac{d^2v}{ds^2} + \Gamma_{11}^2 (\frac{du}{ds})^2 + 2\Gamma_{12}^2 \frac{du}{ds}\frac{dv}{ds} + \Gamma_{22}^2 (\frac{dv}{ds})^2 = 0 \tag{3}$$

where the geodesic arc length is defined by

$$ds = \sqrt{d\bar{R} \cdot d\bar{R}} = \sqrt{E du^2 + 2F du dv + G dv^2}. \tag{4}$$

The parameters used in Equation (4) are defined by

$$E = \overline{R_u} \cdot \overline{R_u}, \tag{5}$$

$$F = \overline{R_u} \cdot \overline{R_v}, \tag{6}$$

$$G = \overline{R_v} \cdot \overline{R_v} \tag{7}$$

where $\overline{R_u}$ and $\overline{R_v}$ represent the partial derivatives of $\bar{R}$ with respect to u and v, respectively. The Christoffel symbols of the second kind Γ^i_{jk} (Reference [2], pg. 202) are given by

$$\Gamma^1_{11} = \frac{GE_u - 2FF_u + FE_v}{2(EG - F^2)}, \tag{8}$$

$$\Gamma^1_{12} = \frac{GE_v - FG_v}{2(EG - F^2)}, \tag{9}$$

$$\Gamma^1_{22} = \frac{2GF_v - GG_u - FG_v}{2(EG - F^2)}, \tag{10}$$

$$\Gamma^2_{11} = \frac{2EF_u - EE_v - FE_u}{2(EG - F^2)}, \tag{11}$$

$$\Gamma^2_{12} = \frac{EG_u - FE_v}{2(EG - F^2)}, \tag{12}$$

$$\Gamma^2_{22} = \frac{EG_v - 2FF_v + FG_u}{2(EG - F^2)} \tag{13}$$

where the subscript u and v denote the partial derivatives with respect to u and v, respectively. After some algebraic manipulation of Equations (2), (3), and (4), the geodesic equation in differential form is obtained as:

$$\frac{d^2u}{dv^2} = \Gamma^2_{11}(\frac{du}{dv})^3 + (2\Gamma^2_{12} - \Gamma^1_{11})(\frac{du}{dv})^2 + (\Gamma^2_{22} - 2\Gamma^1_{12})\frac{du}{dv} - \Gamma^1_{22}, \tag{14}$$

or

$$\frac{d^2v}{du^2} = \Gamma^1_{22}(\frac{dv}{du})^3 + (2\Gamma^1_{12} - \Gamma^2_{22})(\frac{dv}{du})^2 + (\Gamma^1_{11} - 2\Gamma^2_{12})\frac{dv}{du} - \Gamma^2_{22}. \tag{15}$$

In order to solve the above geodesic equations, we need two initial conditions, i.e., $(u, v)|_{s=0}$ and $\frac{du}{dv}|_{s=0}$, where s represents the geodesic arc length on an ellipsoid. The first initial condition specifies the attaching point which lies on the tangential arc defined by the scalar product of the unit normal and the unit vector from the source to the ellipsoid's surface, and the second condition defines the unique geodesic tangent vector which determines a ray path along the ellipsoid's surface.

III. Complete Creeping Wave Paths

As mentioned earlier, all attaching points will lie on the tangential arc on the ellipsoid's surface. The tangential arc for a given source located at (x_s, y_s, z_s) is obtained from the fact that the surface outward normal vector and the incident tangential vector from the source to the ellipsoid surface are orthogonal to each other. The outward surface normal

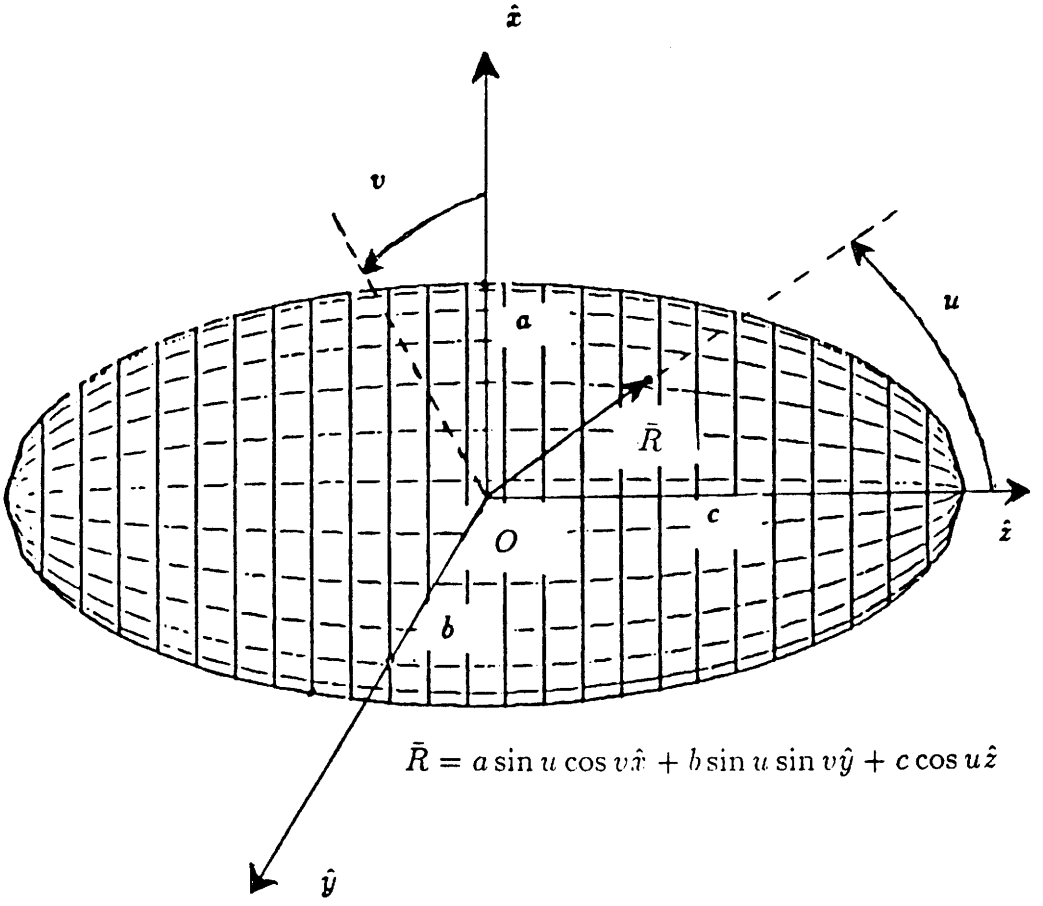

Figure 1: Geometrical configuration of an ellipsoid.

vector on an ellipsoid is

$$\bar{n} = bc\sin u\cos v\hat{x} + ac\sin u\sin v\hat{y} + ab\cos u\hat{z}, \tag{16}$$

and the incident tangential vector from the source to the ellipsoid surface is

$$\bar{t}_i = (a\sin u\cos v - x_s)\hat{x} + (b\sin u\sin v - y_s)\hat{y} + (c\cos u - z_s)\hat{z}. \tag{17}$$

Since $\bar{n}\cdot\bar{t}_i = 0$, we have an equation of the tangential arc, illustrated in Figure 2, as

$$\frac{x_s\sin u\cos v}{a} + \frac{y_s\sin u\sin v}{b} + \frac{z_s\cos u}{c} = 1. \tag{18}$$

Note that all the possible attaching points lie on the arc defined by Equation (18). Let us assume that the field radiated by the source is incident upon a point $(u,v)|_{s=0}$ on this tangential arc. (Note $s = 0$ means that the point is on the tangential arc.)

Now define the incident unit vector $\hat{I}$ as

$$\begin{aligned}\hat{I} &= \frac{\bar{t}_i}{|\bar{t}_i|} = I_x\hat{x} + I_y\hat{y} + I_z\hat{z} \\ &= \frac{(a\sin u\cos v - x_s)\hat{x} + (b\sin u\sin v - y_s)\hat{y} + (c\cos u - z_s)\hat{z}}{\Delta}\end{aligned} \tag{19}$$

where

$$\Delta = \sqrt{(a\sin u\cos v - x_s)^2 + (b\sin u\sin v - y_s)^2 + (c\cos u - z_s)^2}. \tag{20}$$

The first step to determine the appropriate geodesic path is to project the vector $\hat{I}$ onto a finite section of an ellipsoid surface. The projected vector $\overline{I'}$ for the geodesic arc-length Δs is given by

$$\begin{aligned}\overline{I'} &= (R_{ux}\Delta u + R_{vx}\Delta v)\hat{x} + (R_{uy}\Delta u + R_{vy}\Delta v)\hat{y} + (R_{uz}\Delta u + R_{vz}\Delta v)\hat{z} \\ &= I'_x\hat{x} + I'_y\hat{y} + I'_z\hat{z}\end{aligned} \tag{21}$$

where the first subscript u and v represent the partial derivatives of $\bar{R}$ with respect to u and v, respectively, and x, y, and z stand for the x, y, and z components of $\bar{R}_u$ and $\bar{R}_v$, respectively. Solving the above equation for Δu and Δv, we have

$$\begin{aligned}(EG - F^2)\Delta u &= (R_{vx}^2 + R_{vy}^2 + R_{vz}^2)(R_{ux}I'_x + R_{uy}I'_y + R_{uz}I'_z) - \\ &\quad (R_{ux}R_{vx} + R_{uy}R_{vy} + R_{uz}R_{vz})(R_{vx}I'_x + R_{vy}I'_y + R_{vz}I'_z),\end{aligned} \tag{22}$$

$$\begin{aligned}(EG - F^2)\Delta v &= (R_{ux}^2 + R_{uy}^2 + R_{uz}^2)(R_{vx}I'_x + R_{vy}I'_y + R_{vz}I'_z) - \\ &\quad (R_{ux}R_{vx} + R_{uy}R_{vy} + R_{uz}R_{vz})(R_{ux}I'_x + R_{uy}I'_y + R_{uz}I'_z).\end{aligned} \tag{23}$$

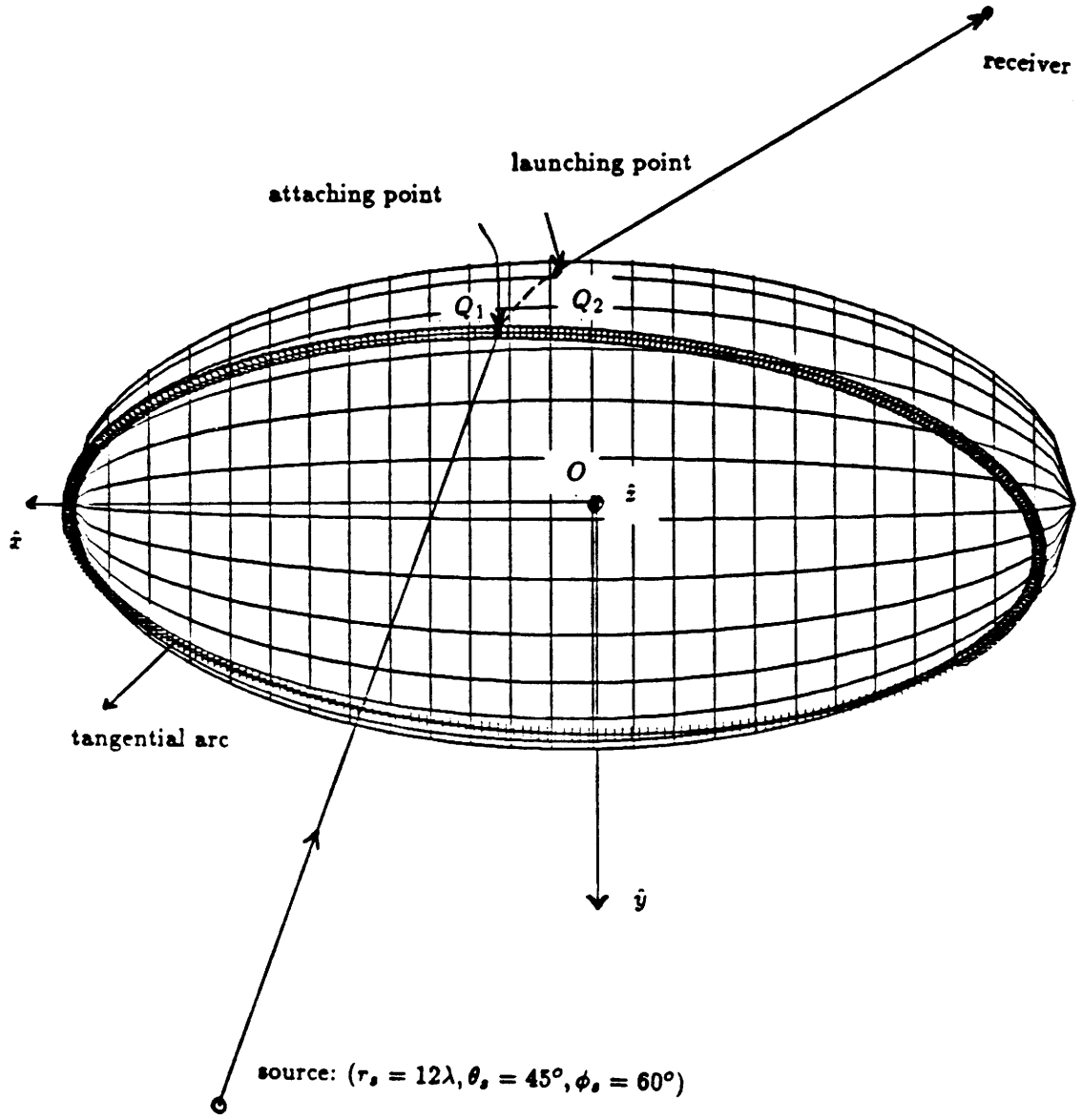

Figure 2: Tangential arc for a source at $(r_s = 12\lambda, \theta_s = 45°, \phi_s = 60°)$. Dimensions of an ellipsoid are $a = 8\lambda$, $b = 4\lambda$, $c = 3\lambda$.

In Equations (22) and (23), I'_x, I'_y, and I'_z can be related to I_x, I_y, and I_z as

$$\frac{I'_y}{I'_x} = \frac{I_y}{I_x}, \tag{24}$$

$$\frac{I'_z}{I'_x} = \frac{I_z}{I_x}. \tag{25}$$

Using the above relationships with Equations (22) and (23), we obtain the first derivative initial condition for the geodesic Equation (14) or (15) as

$$\frac{du}{dv}|_{s=0} = \frac{\Delta u}{\Delta v}|_{s=0} = \frac{T_1}{T_2} \tag{26}$$

where

$$\begin{aligned} T_1 &= (R_{vx}^2 + R_{vy}^2 + R_{vz}^2)(R_{ux} + R_{uy}\frac{I_y}{I_x} + R_{uz}\frac{I_z}{I_x}) - \\ &\quad (R_{ux}R_{vx} + R_{uy}R_{vy} + R_{uz}R_{vz})(R_{vx} + R_{vy}\frac{I_y}{I_x} + R_{vz}\frac{I_z}{I_x}), \\ T_2 &= (R_{ux}^2 + R_{uy}^2 + R_{uz}^2)(R_{vx} + R_{vy}\frac{I_y}{I_x} + R_{vz}\frac{I_z}{I_x}) - \\ &\quad (R_{ux}R_{vx} + R_{uy}R_{vy} + R_{uz}R_{vz})(R_{ux} + R_{uy}\frac{I_y}{I_x} + R_{uz}\frac{I_z}{I_x}). \end{aligned}$$

Once we have the two initial conditions of the attaching point and its first derivative value given by Equation (26), the surface geodesic path on the ellipsoid is uniquely determined. Now the initial search algorithm can be established in the following manner. Let the first derivative $\frac{du}{dv}$ at the jth point along the geodesic path be $\frac{du}{dv}|_j$, then the first derivative at the (j+1)th point (i.e. after the small distance increment along the geodesic) can be approximately obtained using the Taylor series expansion as

$$\frac{du}{dv}|_{j+1} \simeq \frac{du}{dv}|_j + \Delta v \frac{d^2u}{dv^2}|_j, \quad \text{or} \tag{27}$$

$$\frac{dv}{du}|_{j+1} \simeq \frac{dv}{du}|_j + \Delta v \frac{d^2v}{du^2}|_j, \quad \text{if } |\tfrac{dv}{du}| < 1 \tag{28}$$

where $\frac{d^2u}{dv^2}$ and $\frac{d^2v}{du^2}$ are given by Equations (14) and (15), respectively. By increasing the value of v (or u) by a small amount (i.e., dv or du depending on the ratio $|\frac{du}{dv}|$), the geodesic Equation (14) or (15) with Equation (27) or (28) can be solved.

Now our task is to find the four creeping wave paths that will go from source to observer located off the ellipsoid. This is accomplished by first finding a set of creeping rays for the given source and receiver location by a brute force search. In Figure 2, let Q' be the launching (diffraction) point corresponding to the attaching point Q. Just like at the

attaching point, where the incident vector $\hat{I}$ given in equation (19) needs to coincide with the tangent vector of the creeping wave ray at Q, the geodesic tangent unit vector $\hat{t}$ and the vector from the launching point to the receiver $\hat{Q'P}$ must coincide. This can be written as

$$\hat{Q'P} \cdot \hat{t}|_{Q'} = 1. \tag{29}$$

Based on the above fact, the candidate creeping wave paths from a given starting point can be tested for early elimination during the search process by checking the dot product of the geodesic tangent unit vector with a ray from the local creeping wave point to the receiver. If this quantity is converging to unity the search process is continued. If it starts to diverge, the process is stopped and the next starting point along the geodesic tangent arc is chosen and tried. The detailed description of the criteria for the search algorithm is well documented in [6]. Once four paths are found the search stops and the parameters for the UTD field calculations such as the energy spreading factor, attenuation factor, and the caustic distance at the diffraction point are evaluated numerically. Note that this initial searching algorithm needs to be reinitiated if the receiver goes into (or comes out of) the shadow region, or goes through a caustic region.

Once a given set of creeping wave paths for the initial source and receiver location are known, the entire ellipsoid need not be searched. The next set of rays corresponding to a new observation point is found using a bisectional search. The method proceeds by looking at a tangent start location on either side of the known path. The signs of convergence are checked. Once the direction is known, another point is taken on the correct side a small amount over or half way in between paths previously chosen until the right path is found. A given path is normally found in about four tries. This is done for all four paths. This can speed up the solution by a very significant amount. Our experience is a speed up of around 20 times over the brute force search used for the entire pattern cut.

IV. Numerical Examples of Geodesic Paths on an Ellipsoid

In Figure 3, the geodesic path for a source located at $(r_s = 12\lambda, \theta_s = 45°, \phi_s = 60°)$ is shown. In this figure, the starting (attaching) point on the tangential arc is defined by $v_s = 135°$ and $u_s = 90°$. The dimension of ellipsoid is $8\lambda \times 4\lambda \times 3\lambda$. In Figure 4, four complete ray paths for the given source located at $(r_s = 12\lambda, \theta_s = 45°, \phi_s = 180°)$

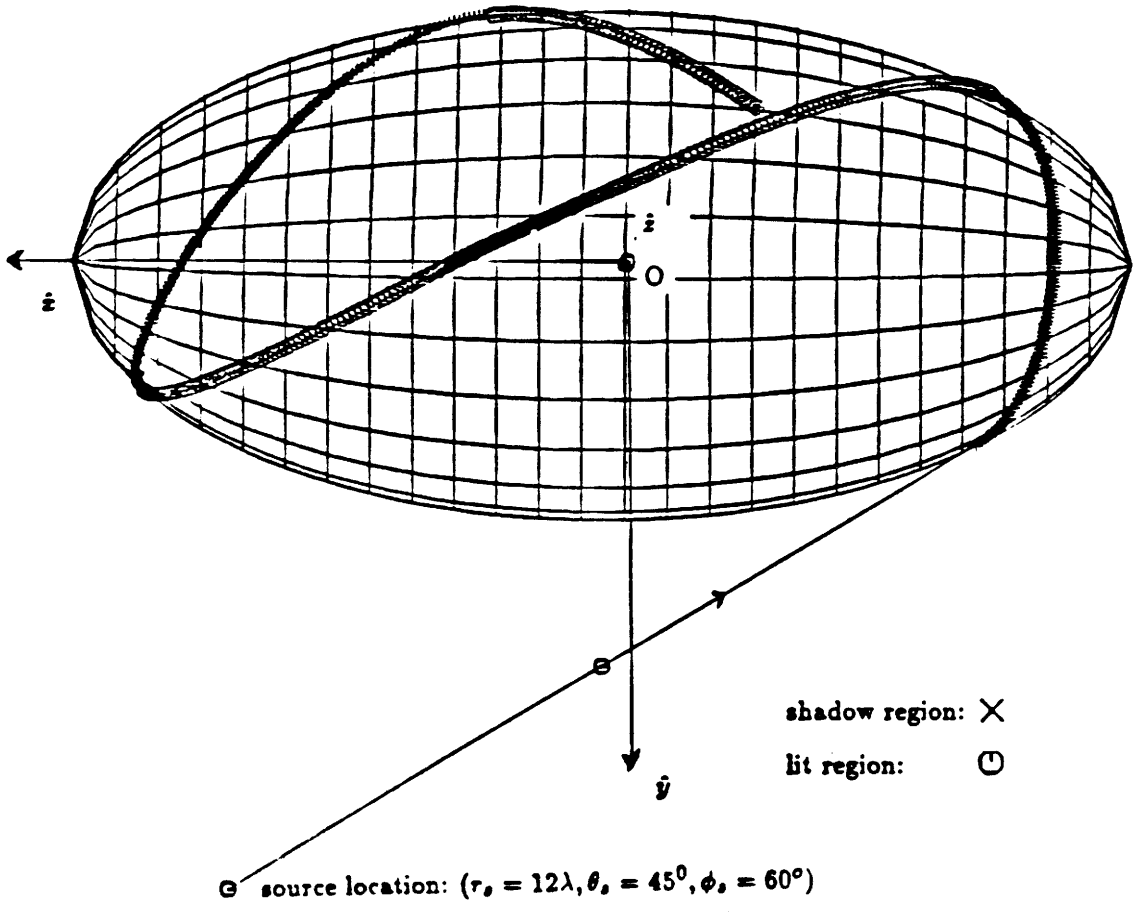

Figure 3: Geodesic path on a $a = 8\lambda, b = 4\lambda, c = 3\lambda$ ellipsoid. Attaching point is defined by $v_s = 135°, u_s = 90°$.

and receiver located at $(r_o = 8\lambda, \theta_o = 135°, \phi_o = 0°)$ are presented. The ellipsoid has a dimension of $4\lambda \times 2\lambda \times 1\lambda$.

In order to verify the present approach, comparisons are made between the present results and calculated data given in [4]. Figure 5 shows the geodesic tangent defined by the radial vector direction (θ_t, ϕ_t) for a given γ on $4\lambda \times 6\lambda \times 40\lambda$ ellipsoid. The definitions for the radial vector parameters (θ_t, ϕ_t) and γ are illustrated in Figures 6(a) and 6(b), respectively. Note that the parameter ζ in Figure 5 is the argument of the Pekeris' Caret functions [7]. The solid line represent the perturbation method [4], the dotted line is for the integral form of the geodesic equation [4], and the black dots are for the present approach. There exists good agreement between the present approach and the solution using the integral form of the geodesic equation. Comparisons of the geodesic paths defined by the surface parameters (θ_Q, ϕ_Q) for given γ on $2\lambda \times 3\lambda \times 20\lambda$ ellipsoid are made in Figure 7.

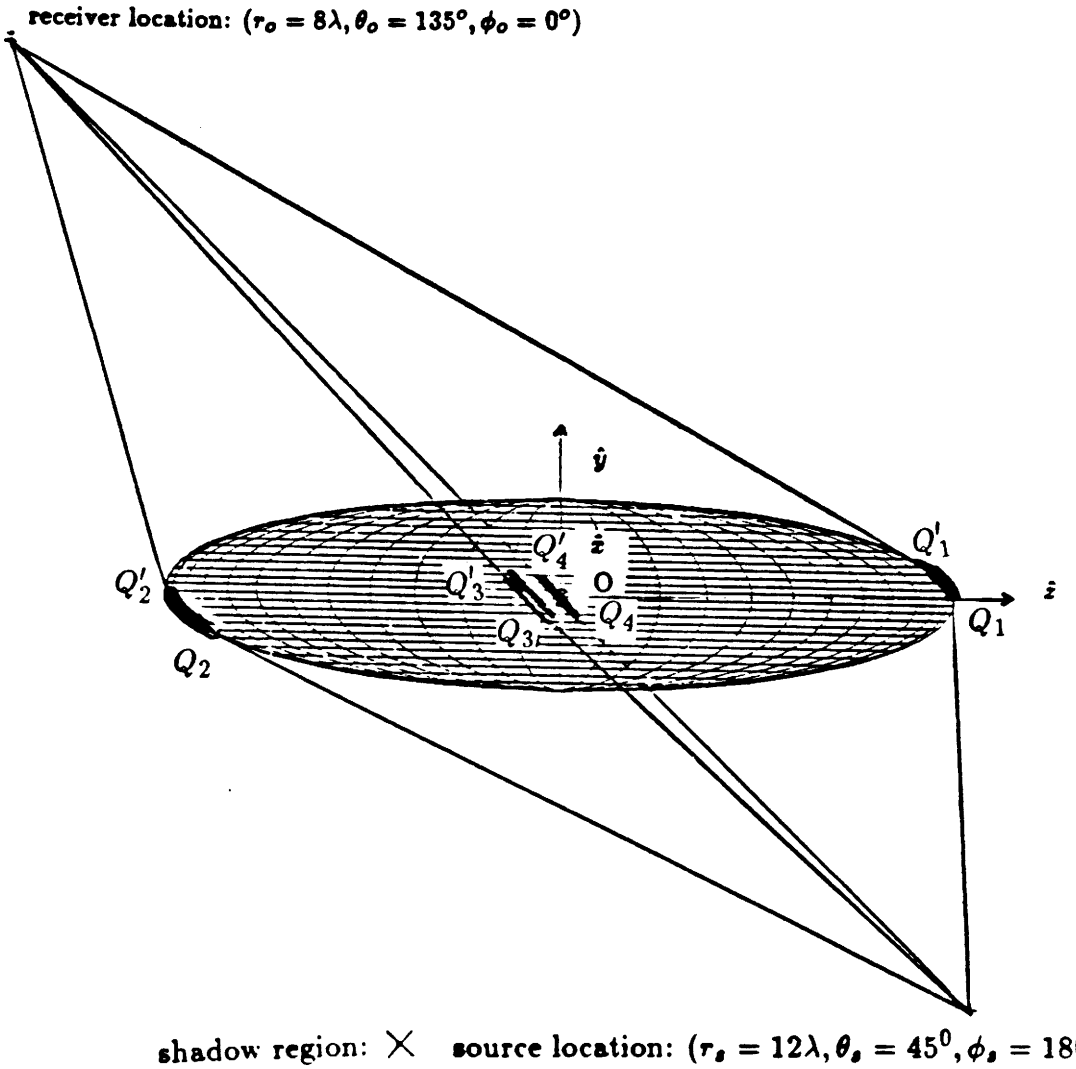

Figure 4: Four creeping wave paths for a given source and receiver location on a $4\lambda \times 2\lambda \times 1\lambda$ ellipsoid.

The surface parameters (θ_Q, ϕ_Q) are illustrated in Figure 6(c). There also exists excellent agreement among results.

V. Determination of the Energy Spreading Factor and Caustic Distance

In the calculation of the UTD creeping wave, the proper values of the energy spreading factor $(\sqrt{\frac{d\eta_1}{d\eta_2}})$ and caustic distance at the diffraction point (ρ_2^d) play important roles for not only the amplitude but also the phase of the creeping wave. In general these quantities are not easy to determine. In this section, a numerical method to determine these parameters are described based on the differential geometry information readily obtained in the complete ray path section.

A coordinate system in which the parameter curves are orthogonal to each other, and one of the families of parameter curves is geodesic, is called a set of geodesic coordinates. Let the s- parameter curves be geodesics and w-parameter curves be orthogonal to the s-parameter curves. Now we define $\overline{X} = \overline{X}(s, w)$ as the vector notation of an arbitrary arc on a surface. In general, if the two parameter curves on a patch are orthogonal, the Gaussian curvature K is given by

$$K = \frac{-1}{\sqrt{EG}}\left[\frac{\partial}{\partial s}\left(\frac{1}{\sqrt{E}}\frac{\partial\sqrt{G}}{\partial s}\right) + \frac{\partial}{\partial w}\left(\frac{1}{\sqrt{G}}\frac{\partial\sqrt{E}}{\partial E}\right)\right], \tag{30}$$

where

$$E = \frac{\partial\overline{X}(s,w)}{\partial s}\cdot\frac{\partial\overline{X}(s,w)}{\partial s}, \tag{31}$$

$$G = \frac{\partial\overline{X}(s,w)}{\partial w}\cdot\frac{\partial\overline{X}(s,w)}{\partial w}. \tag{32}$$

If $\overline{X}(s, w)$ is a set of geodesic coordinates on a surface of class ≥ 3 such that s-parameter curves are geodesics and s is a natural parameter, then E=1 and Equation (30) becomes

$$K(s) = \frac{-1}{\sqrt{G}}\frac{d^2\sqrt{G}}{ds^2} \tag{33}$$

where $K(s)$ is a Gaussian curvature along the geodesic path, which is a product of the two principal curvatures. By noticing that parameter curves are geodesics, one can interpret $\sqrt{G}$ as the surface ray tube width which is orthogonal to the geodesic. Namely, $\sqrt{G}$ in Equation (33) is the quantity of our interest to evaluate the energy spreading factor. Since

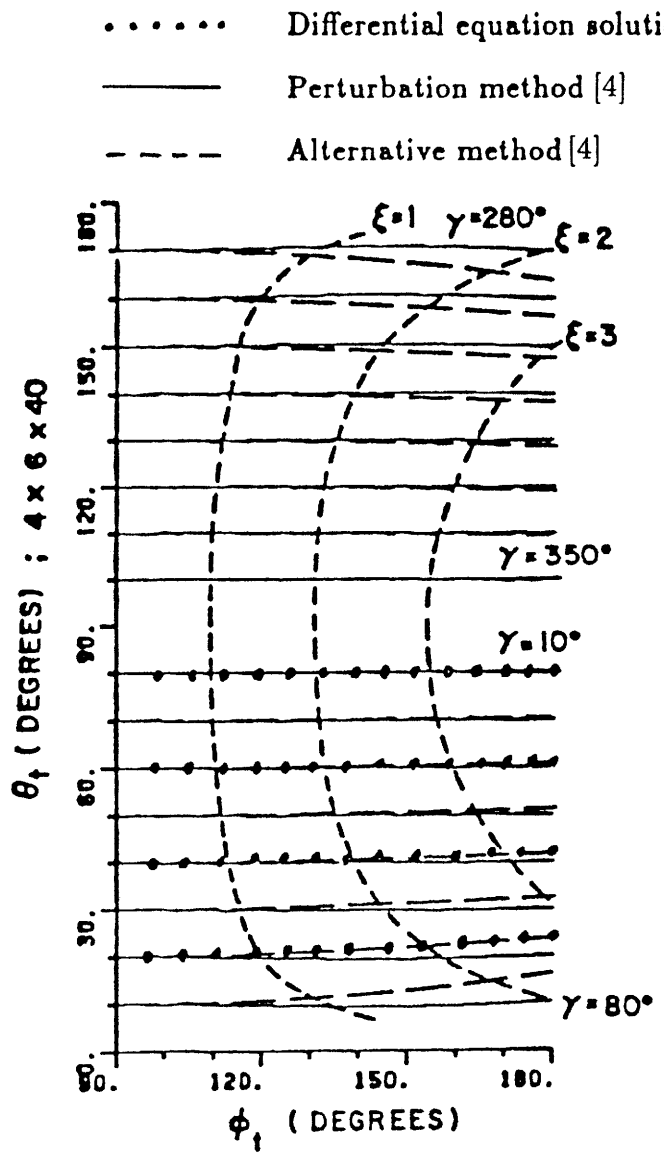

Figure 5: Comparison of the geodesic tangent defined by the radial vector direction (θ_t, ϕ_t) for given γ on a $4\lambda \times 6\lambda \times 40\lambda$ ellipsoid.

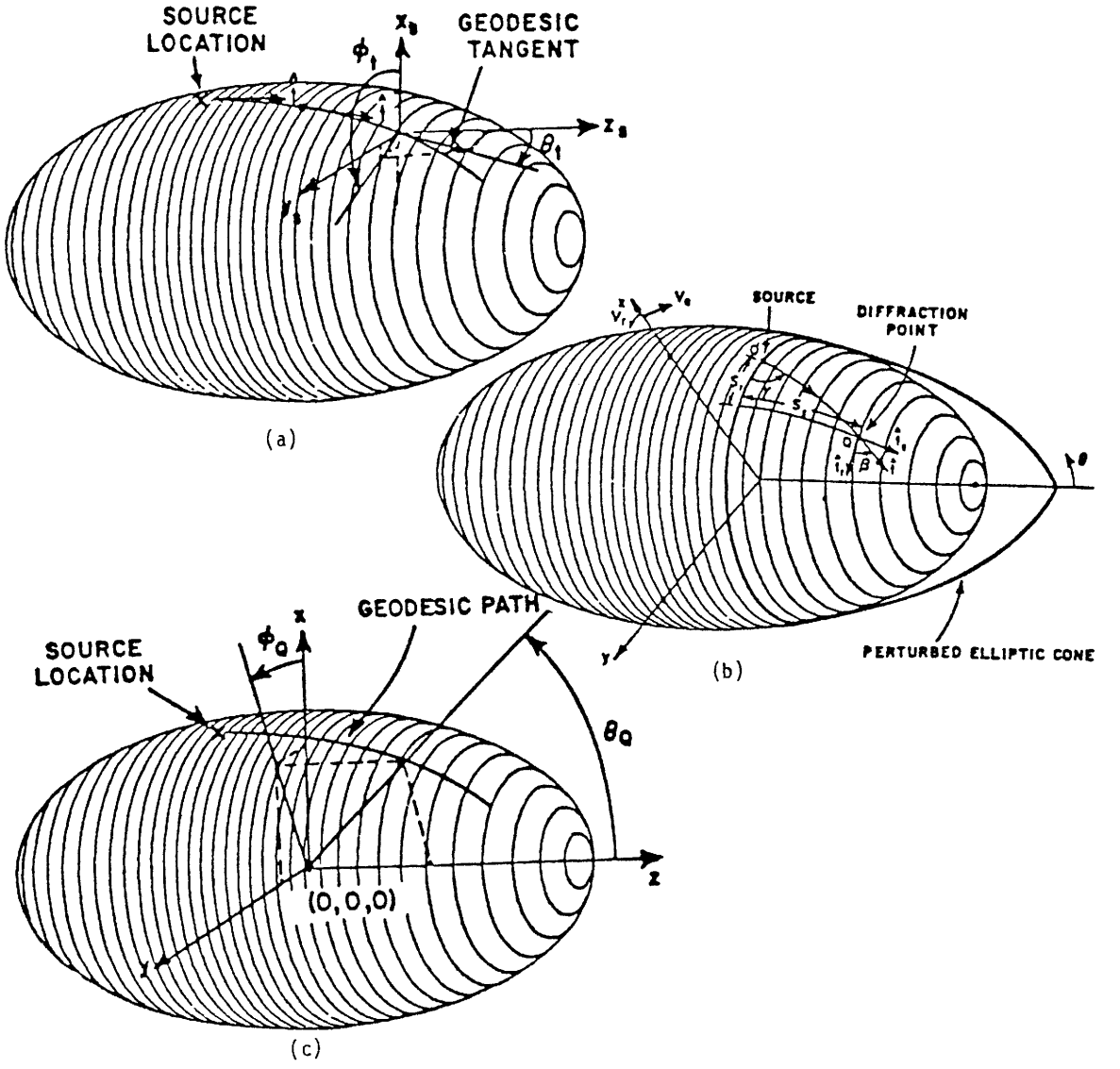

Figure 6: Illustration of the relationship of a geodesic path to various parameters defined in Reference [4]: (a). surface parameters (θ_t, ϕ_t). (b). angle γ for the elliptic cone perturbation. (c). surface parameters (θ_Q, ϕ_Q).

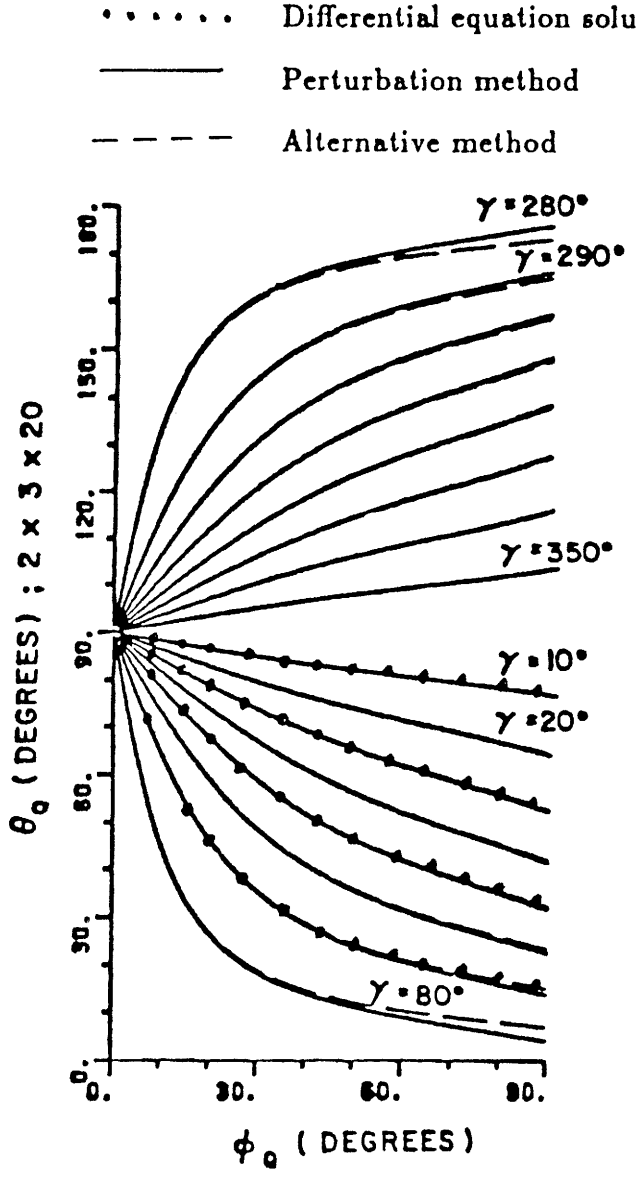

Figure 7: Comparison of the geodesic paths defined by the surface parameters (θ_Q, ϕ_Q) for given γ on a $2\lambda \times 3\lambda \times 20\lambda$ ellipsoid.

Equation (33) is a second order differential equation, we need two initial conditions. They are given by

$$\sqrt{G}|_{s=0} = 1, \text{ and} \tag{34}$$

$$\frac{d\sqrt{G}}{ds}|_{s=0} = K_t = \frac{1}{R_t} \tag{35}$$

where s represents the geodesic arc length and R_t is the transverse radius of curvature of the incident wavefront at the incident shadow boundary in the plane tangent to the surface.

Let $y = \sqrt{G}$, then Equation (33) can be written as

$$\frac{d^2y}{ds^2} + K(s)y = 0 \tag{36}$$

with the two initial conditions

$$y|_{s=0} = 1 \tag{37}$$

$$\frac{dy}{ds}|_{s=0} = K_t. \tag{38}$$

Let Q be the initial (i.e., attaching) point and Q' be the launching (diffraction) point on the surface. If we know the value of y at the present location (i.e., nth point) along the geodesic path, then the value of y at (n+1)th point (i.e., after making Δs increment from nth point along the geodesic) can be obtained by keeping terms up to second order in the Taylor series expansion as

$$y_{n+1} \simeq y_n + (\Delta s)y'_n + \frac{(\Delta s)^2}{2}y''_n, \tag{39}$$

$$y'_{n+1} \simeq y'_n + (\Delta s)y''_n \tag{40}$$

where the prime($'$) represents the derivative with respect to the geodesic arc length s. Finally, the energy spreading factor $\sqrt{\frac{d\eta_1}{d\eta_2}}$ is given by

$$\sqrt{\frac{d\eta_1}{d\eta_2}} = \sqrt{\frac{y|_{s=0}}{y|_{Q'}}} = \sqrt{\frac{1}{\sqrt{G}|_{Q'}}}. \tag{41}$$

Since the surface ray tube at the diffraction point Q' can be localized, as shown in Figure 8 , we have

$$\frac{\rho_2^d}{d\eta} = \frac{\rho_2^d - \Delta s}{d\eta_o}. \tag{42}$$

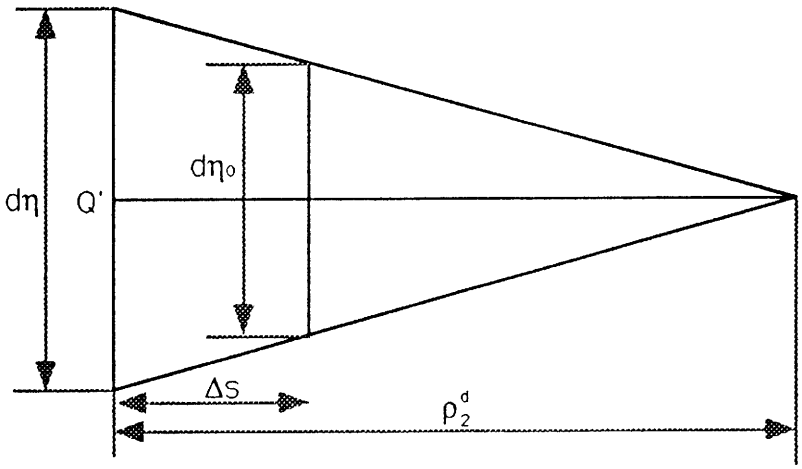

Figure 8: Local geometry for the calculation of ρ_2^d at the diffraction point Q'.

By replacing y_{n+1} to $d\eta$ and y_n to $d\eta_o$ in Equation (39),

$$d\eta \simeq d\eta_o + (\Delta s) d\eta_o' + \frac{(\Delta s)^2}{2} d\eta_o''. \tag{43}$$

By solving Equations (42) and (43) for ρ_2^d, the caustic distance at the diffraction point is obtained approximately as

$$\rho_2^d \simeq \frac{d\eta_o + d\eta_o' \Delta s + d\eta_o'' \frac{\Delta s^2}{2}}{d\eta_o' + d\eta_o'' \frac{\Delta s}{2}}. \tag{44}$$

The parameters used in Equation (44) are defined as
$d\eta$: surface ray tube width at the diffraction point Q',
$d\eta_o$: surface ray tube width at $(s_{Q'} - \Delta s)$,
$d\eta_o'$: the derivative of $d\eta_o$ with respect to s,
$d\eta_o''$: the second derivative of $d\eta_o$ with respect to s, and
Δs is the incremental step size of the geodesic arc length.

VI. Conclusion

Numerical techniques to determine the UTD creeping wave path for the bistatic scattering of an ellipsoid is investigated. Also the energy spreading factor of the creeping wave and caustic distance at the diffraction point are obtained in terms of the differential geometry information furnished by tracing the ray path from the source to the surface geodesic then

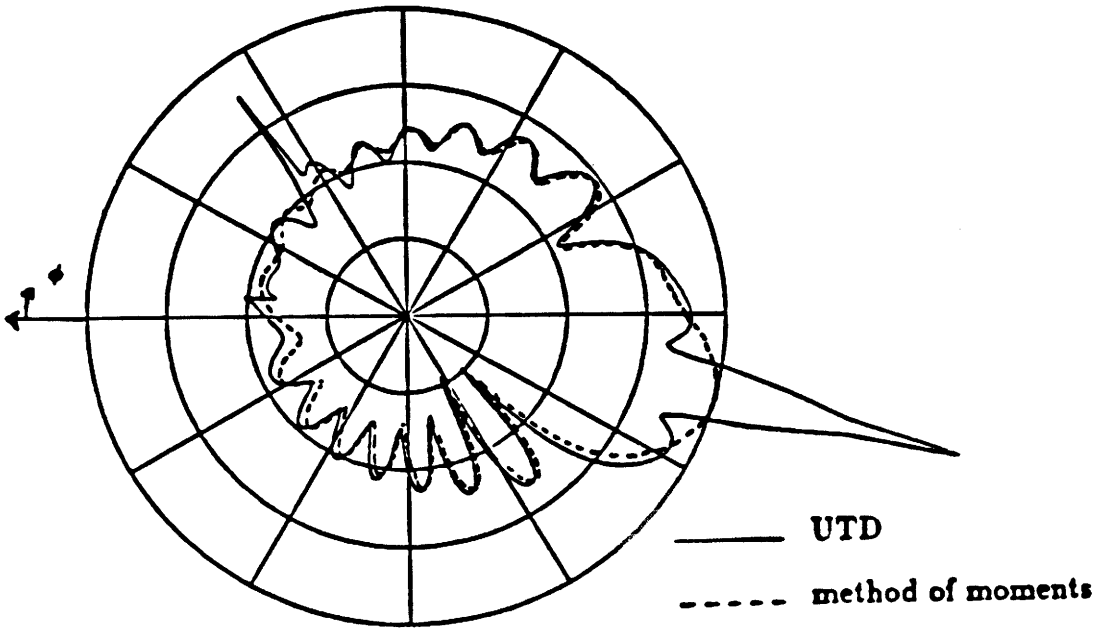

Figure 9: Far zone bistatic scattered field of a $2\lambda \times 1\lambda \times 1\lambda$ spheroid with E-plane polarization with the incident field fixed at $(\theta_s = 90°, \phi_s = 15°)$ and the pattern taken in the $\theta_o = 90°$ plane. The scale is in 10 dB steps.

to the receiver off the surface. Some geodesic paths on an ellipsoid for a given source and receiver location pair are calculated and compared to the data obtained by other methods [4]. There exists good agreement among them. The approach developed can provide about a factor of 20 speed improvement over a brute force way of finding the creeping wave paths.

The numerical methods described in the previous sections are not only valid for an ellipsoid but also applicable to a general doubly curved surface. The major change is in determining the original attaching points. For a general surface, this may require a slow search process. The key point, however, is that the solution can be greatly speeded up by using a bisectional search for the subsequent ray paths.

When these numerical methods are applied to calculate the UTD bistatic scattering patterns of an ellipsoid, a sphere, and a spheroid [5,6], there exists good agreement between the UTD results (present numerical approach) and exact or body of revolution method of moments results except for the caustic regions. As an example of this, the far zone bistatic scattered field pattern of a $2\lambda \times 1\lambda \times 1\lambda$ spheroid is shown in Figure 9. The polarization is parallel to the plane of incidence. The field is incident from a fixed direction of $(\theta_s = 90°, \phi_s = 15°)$. The observer is at $(\theta_o = 90°, \phi_o = \phi)$. The UTD results are

compared to a body of revolution method of moments code. There is excellent agreement except at the forward scattering caustic of $\phi = 135°$ and the local caustic where one of the creeping wave ray tube spread factors converges at around $\phi = 50°$ in the pattern.

References

[1] P. H. Pathak, W. D. Burnside, and R. J. Marhefka, "A Uniform GTD Analysis of the Diffraction of Electromagnetic Waves by a Smooth Convex Surface," *IEEE* Trans. on Antennas and Propagation, Vol. AP-28, No. 5, pp 631-642, Sept. 1982.

[2] M. M. Lipschutz, *Differential Geometry*, Schaum's Outline Series, McGraw-Hill Book Co., N.Y., 1969.

[3] R. L. Barger and M. S. Adams, "Semianalytic Modeling of Aerodynamic Shapes," NASA technical Paper 2413, 1985, NASA Langley Research Center, Hampton, Virginia.

[4] J. G. Kim, N. Wang, and C. D. Chuang, "Geodesic Paths of an Ellipsoid Mounted Antenna," Technical Report 713321-3, March 1982, the Ohio State University ElectroScience Laboratory, Dept. of Electrical Engineering; prepared under Contract No. N00019-80-PR- RJ015 for Naval Air Systems Commands.

[5] J. Choi, "Bistatic Scattering Analysis of an Ellipsoid", Ms. Thesis, The Ohio State University, Department of Electrical Engineering, Columbus, Ohio, 1986.

[6] J. Choi and R. J. Marhefka, "Bistatic Scattering Analysis of an Ellipsoid," Technical Report 717674-2, Nov. 1986, the Ohio State University ElectroScience Laboratory, Department of Electrical Engineering; prepared under Contract No. N60530-85-C- 0249 for Naval Weapons Center.

[7] N. A. Logan, "General Research in Diffraction Theory," Vol. 1, LMSD-288087 and Vol. 2, LMSD-288088, Missile and Space Division, Lockheed Aircraft Corporation, December 1957.